

Nonstationary distributed axisymmetric load on an elastic half-space

Veniamin D. Kubenko · Igor V. Yanchevsky

Received: 5 April 2014 / Accepted: 22 December 2014 / Published online: 24 April 2015
© Springer Science+Business Media Dordrecht 2015

Abstract This paper presents analytical and numerical-analytic approaches to solving the problem of the action of an arbitrarily distributed axisymmetric load applied instantly to the surface of an isotropic elastic half-space. The first approach is built around the Laplace and Hankel integral transforms whose inversion is performed jointly with Cagniard's technique, and as a result, exact analytical expressions are obtained for computing stresses along an axis of symmetry. The second approach uses the Laplace integral transform and the expansion of sought for values into the Fourier–Bessel series to reduce the problem to a numerical solution of a series of Volterra integral equations. Concrete numerical analysis was performed for cases where the domain of application of a distributed load is fixed or expands in time with both constant and variable velocity.

Keywords Analytic solution · Distributed axisymmetric load · Elastic half-space · Fourier–Bessel expansion · Laplace transform · Nonstationary problem

Mathematics Subject Classification 35C10 · 44A30 · 45D05 · 74H10 · 74J10

1 Introduction

Studies in wave processes in an isotropic elastic half-space with an application of axisymmetric surface actions, in particular, distributed normal mechanical loads, have been the subject of investigation in quite a number of papers. Their bibliographies are given in [1–5]. For their solution, besides implementing classical numerical methods (the finite-difference [6] and finite-element methods [7]), effective numerical-analytic methods have been developed. They are based on integral transforms – Laplace in time and Hankel in space. The methods of building originals are different, and they depend primarily on the law of load space-time distribution on the half-space boundary.

In some studies, asymptotic methods are used for transforms, and the features of displacement and stress fields near wave fronts have been investigated (see [8,9]). The methods of the theory of residues in [10] applied to a Hertz distribution type load, which occurs under a smooth flat die in the static load contact problem, have yielded expressions for normal displacements of half-space surface points as multiple integrals of real variable functions. The displacements of points on a half-space surface and the axis of symmetry were also studied in [11,12], where,

V. D. Kubenko · I. V. Yanchevsky (✉)
S.P. Tymoshenko Institute of Mechanics of National Academy of Science of Ukraine, 3 Nesterova Str., Kiev 03057, Ukraine
e-mail: yanchevsky@ukr.net

for joint transform inversion, the Cagniard–de Hoop technique [13] was implemented taking into account transform homogeneity with respect to transform parameters. For an approximate search for variables distant from the points' axis of symmetry, the study by [11] used the saddle technique for computing the Laplace inverse transform integral because immediate implementation of the Cagniard technique for the Laplace inverse transform integral containing the Bessel function is mathematically challenging. Similar to [11], the paper [14] presents solutions for displacements and stresses in the inner points of the half-space for cases where an evenly distributed load with a stepwise profile in time is applied to its boundary. Corresponding expressions have been obtained as a sum of nine indefinite integrals treated as “static,” “Rayleigh,” and “dynamic” components. In studying stresses in points on the axis of symmetry, the introduction of new integration variables reduced double indefinite integrals containing Bessel functions to definite integrals of elementary functions. The computation involves special quadrature formulas to account for kernel singularity. The paper [15] offered another approach to finding displacements of half-space points. Computational expressions are written both in the form of a superposition of analytical solutions of the Lamb problem and as a convolution over the radial coordinate of the external load distribution function and the corresponding fundamental solution. In so doing, the researchers considered two kinds of load distribution over the spatial coordinate, and elastic displacements were computed for a delta function time-variable load. The latter caused a jump in calculated displacements, which does not correlate with the linear formulation of the mechanics of continua.

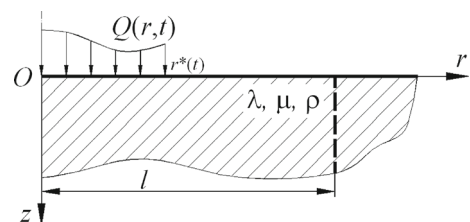
In the aforementioned studies, the load application domain is fixed. Problems with a variable application domain are less well understood. Published studies investigate primarily the cases of even extension of boundaries, and the displacement of points is investigated either on the half-space surface or in proximity to elastic wave fronts [8, 16].

As the preceding analysis shows, analytical solutions of the nonstationary problem in the action of a surface axisymmetric load on an elastic isotropic half-space have been obtained only for certain partial cases of load space-time distribution. This paper presents a numerical-analytic approach to investigating stress and displacement fields in an elastic half-space when a nonstationary axisymmetric arbitrary-profile load is applied to its boundary. The method is built around the time-variable Laplace transform and the expansion of variables in the Fourier–Bessel series over the radial coordinate of a model cylinder. This eliminates the need for an involved inversion of two integral transforms. Note that this approach is similar to that in [17] as applied to solving the problem in elastic medium shock with a blunt body. In addition, the paper describes an analytical technique for determining stresses in points on the axis of symmetry for a moving boundary of the load distribution domain. The method is built around Laplace and Hankel integral transforms, whereas the transition to the domain of original functions is performed exactly using the Cagniard–de Hoop method. The computations performed with both approaches were compared with one another and the results of other authors. Comparison has shown that the computations demonstrate the required accuracy and can be used for a wide range of acting loads.

2 Problem statement

An elastic half-space, to which a nonstationary load is applied, is considered. The physical properties of the half-space material are described using elastic Lamé constants (λ and μ) and density ρ . The problem has axial symmetry; therefore, the half-space is related to the cylindrical coordinate system Orz selected such that the Oz -axis, being the axis of symmetry, is directed to the half-space, and the Or -axis is directed along its surface (Fig. 1).

Fig. 1 Scheme of half-space loading



The nonstationary load in the form of normal stress occurs at a certain initial time instant $t = 0$ and, in general, is a function of time and coordinate r .

The following dimensionless variables and notations are introduced:

$$\bar{r} = \frac{r}{R}, \quad \bar{z} = \frac{z}{R}, \quad \bar{u}_j = \frac{u_j}{R}, \quad \bar{t} = \frac{c_p t}{R}, \quad \bar{\sigma}_{jk} = \frac{\sigma_{jk}}{\lambda + 2\mu} \quad (j, k = r, z), \quad \alpha = 1, \quad \beta = \frac{c_s}{c_p}. \tag{1}$$

Here, R is a certain characteristic linear size, u_j projections of the elastic displacements vector, σ_{jk} stress tensor components, and $c_p = \sqrt{(\lambda + 2\mu)/\rho}$ and $c_s = \sqrt{\mu/\rho}$ compression and shear wave propagation velocities, respectively. In what follows, we shall use only dimensionless notations; hence, their overline shall be omitted.

The motion of an elastic medium in the axisymmetric case is described by two scalar wave potentials, Φ and Ψ , satisfying the following equations [18]:

$$\Delta \Phi = \frac{1}{\alpha^2} \frac{\partial^2 \Phi}{\partial t^2}, \quad \Delta \Psi = \frac{1}{\beta^2} \frac{\partial^2 \Psi}{\partial t^2}, \quad \Delta \equiv \frac{\partial^2}{\partial r^2} + \frac{1}{r} \frac{\partial}{\partial r} + \frac{\partial^2}{\partial z^2}. \tag{2}$$

Physical values (displacements and stresses) are expressed by the potentials Φ and Ψ as follows:

$$\begin{aligned} u_r &= \frac{\partial \Phi}{\partial r} + \frac{\partial^2 \Psi}{\partial r \partial z}, & u_z &= \frac{\partial \Phi}{\partial z} - \frac{\partial^2 \Psi}{\partial r^2} - \frac{1}{r} \frac{\partial \Psi}{\partial r}, \\ \sigma_{zz} &= \left(1 - 2\frac{\beta^2}{\alpha^2}\right) \frac{\partial^2 \Phi}{\partial t^2} + 2\beta^2 \left(\frac{\partial^2 \Phi}{\partial z^2} - \frac{\partial^3 \Psi}{\partial r^2 \partial z} - \frac{1}{r} \frac{\partial^2 \Psi}{\partial r \partial z}\right), \\ \sigma_{rr} &= \left(1 - 2\frac{\beta^2}{\alpha^2}\right) \frac{\partial^2 \Phi}{\partial t^2} + 2\beta^2 \left(\frac{\partial^2 \Phi}{\partial r^2} + \frac{\partial^3 \Psi}{\partial r^2 \partial z}\right), \\ \sigma_{rz} &= 2\beta^2 \frac{\partial}{\partial r} \left(\frac{\partial \Phi}{\partial z} + \frac{\partial^2 \Psi}{\partial z^2} - \frac{1}{2\beta^2} \frac{\partial^2 \Psi}{\partial t^2}\right). \end{aligned} \tag{3}$$

The boundary conditions on the surface $z = 0$ consist in specifying the normal stress σ_{zz} and an absence of shearing stress σ_{zr} :

$$\sigma_{zz}|_{z=0} = Q(r, t), \quad \sigma_{zr}|_{z=0} = 0 \quad (r \geq 0). \tag{4}$$

The initial conditions for potentials are zero conditions:

$$\Phi|_{t=0} = \dot{\Phi}|_{t=0} = \Psi|_{t=0} = \dot{\Psi}|_{t=0} = 0, \tag{5}$$

and at infinity, wave perturbations decay.

3 Analytical solution

The solution of problem (1)–(5) is obtained using a Laplace integral transform for time t with parameter s and a Hankel integral transform of order 0 for coordinate r with parameter ξ [19]. In particular,

$$\begin{aligned} f^L(s) &= L\{f(t)\} = \int_0^\infty e^{-st} f(t) dt, \\ f(t) &= L^{-1}\{f^L(s)\} = \frac{1}{2\pi} \int_{\delta-i\infty}^{\delta+i\infty} e^{ts} f^L(s) ds, \end{aligned} \tag{6}$$

$$f^B(\xi) = B\{f(r)\} = \int_0^\infty f(r)J_0(r\xi)r \, d\xi,$$

$$f(r) = B^{-1}\{f^B(\xi)\} = \int_0^\infty f^B(\xi)J_0(r\xi)\xi \, d\xi.$$

Here, L and B denote, respectively, Laplace and Hankel integral transform operators, L^{-1} and B^{-1} are inversion operators, and J_m is the cylindrical Bessel function of the first kind for index m . The function transform is denoted by the corresponding upper index. In the space of Laplace and Hankel transforms [19], we obtain the following boundary problem (in which the initial conditions have been realized):

$$\frac{\partial^2 \Phi^{LB}}{\partial z^2} - \left(\frac{s^2}{\alpha^2} + \xi^2\right)\Phi^{LB} = 0, \quad \frac{\partial^2 \Psi^{LB}}{\partial z^2} - \left(\frac{s^2}{\beta^2} + \xi^2\right)\Psi^{LB} = 0,$$

$$\left(1 - 2\frac{\beta^2}{\alpha^2}\right)s^2\Phi^{LB} + 2\beta^2\left(\frac{\partial^2 \Phi^{LB}}{\partial z^2} + \xi^2\frac{\partial \Psi^{LB}}{\partial z}\right) = Q^{LB}(s, \xi) \quad (z = 0),$$

$$\frac{\partial \Phi^{LB}}{\partial z} + \frac{\partial^2 \Psi^{LB}}{\partial z^2} - \frac{s^2}{2\beta^2}\Psi^{LB} = 0 \quad (z = 0),$$

$$\Phi^{LB} \rightarrow 0; \quad \Psi^{LB} \rightarrow 0 \quad (z \rightarrow \infty).$$
(7)

The general solution of wave equations decaying at $z \rightarrow \infty$ has the form

$$\Phi^{LB} = Ae^{-(z/\alpha)P}, \quad P = \sqrt{s^2 + \alpha^2\xi^2}, \quad \Psi^{LB} = Be^{-(z/\beta)S}, \quad S = \sqrt{s^2 + \beta^2\xi^2}. \quad (8)$$

By determining the arbitrary constants A and B from the boundary conditions, we shall obtain an expression for the normal stress transform:

$$\sigma_{zz}^{LB}(\xi, s, z) = Q^{LB}(\xi, s) \frac{(s^2 + 2\beta^2\xi^2)^2 e^{-(z/\alpha)P} - 4\frac{\beta^3}{\alpha}\xi^2 P S e^{-(z/\beta)S}}{(s^2 + 2\beta^2\xi^2)^2 - 4\frac{\beta^3}{\alpha}\xi^2 P S}. \quad (9)$$

Displacement u_z and shear stress σ_{rz} in transforms are written as follows:

$$u_z^{LB} = -Q^{LB}(\xi, s) \frac{1}{\alpha} \frac{P[(s^2 + 2\beta^2\xi^2)e^{-(z/\alpha)P} - 2\beta^2\xi^2 e^{-(z/\beta)S}]}{(s^2 + 2\beta^2\xi^2)^2 - 4\frac{\beta^3}{\alpha}\xi^2 P S},$$

$$\sigma_{rz}^{LB} = -Q^{LB}(\xi, s) \frac{1}{\alpha} \frac{(s^2 + 2\beta^2\xi^2)P[e^{-(z/\alpha)P} - e^{-(z/\beta)S}]}{(s^2 + 2\beta^2\xi^2)^2 - 4\frac{\beta^3}{\alpha}\xi^2 P S}. \quad (10)$$

Now the problem consists of inversion of expressions obtained with respect to integral transforms.

Note that the fraction in (9)–(10) is a homogeneous function of transform parameters s and ξ . For certain types of external actions, which define the function $Q^{LB}(s, \xi)$, this makes it possible to obtain analytical expressions for σ_{zz} , σ_{rz} , and u_z using the Cagniard technique [13] of joint inversion of integral transforms. The inversion technique depends on the properties of the function $Q^{LB}(\xi, s) = LB\{Q(r, t)\}$. Hence, it should be made more specific. Here we shall investigate a load of the following kind:

$$Q(r, t) = q_0 H(t) H(kt - r), \quad (11)$$

where H is the Heaviside step function.

Function (11) specifies the normal stress that occurs spontaneously and propagates at a constant velocity over the half-space surface. It is not difficult to determine the Fourier and Hankel transforms for this function:

$$Q^L(r, s) = q_0 \frac{1}{s} e^{-s(r/k)}, \quad Q^{LB}(\xi, s) = q_0 \frac{k^2}{(s^2 + \xi^2 k^2)^{3/2}}. \tag{12}$$

Then, for example, (9) yields

$$\sigma_{zz}^{LB}(\xi, s, z) = q_0 k^2 \frac{(s^2 + 2\beta^2 \xi^2)^2 e^{-(z/\alpha)P} - 4 \frac{\beta^3}{\alpha} \xi^2 P S e^{-(z/\beta)S}}{(s^2 + \xi^2 k^2)^{3/2} \left[(s^2 + 2\beta^2 \xi^2)^2 - 4 \frac{\beta^3}{\alpha} \xi^2 P S \right]}.$$

We perform a Hankel transform inversion for the z -axis,

$$\sigma_{zz}^L(r = 0, s, z) = q_0 k^2 \int_0^\infty \frac{(s^2 + 2\beta^2 \xi^2)^2 e^{-(z/\alpha)P} - 4 \frac{\beta^3}{\alpha} \xi^2 P S e^{-(z/\beta)S}}{(s^2 + \xi^2 k^2)^{3/2} \left[(s^2 + 2\beta^2 \xi^2)^2 - 4 \frac{\beta^3}{\alpha} \xi^2 P S \right]} \xi d\xi, \tag{13}$$

and, assuming s is real, we shall change the variable: $\xi = s\eta$, $d\xi = sd\eta$.

Let us rewrite (13) as the sum of two integrals:

$$\sigma_{zz}^L(s, z) = \frac{q_0}{s} \left[R_1^L(s, z) + R_2^L(s, z) \right] = \frac{q_0}{s} \left[\int_0^\infty \bar{R}_1^L(s, z, \eta) d\eta + \int_0^\infty \bar{R}_2^L(s, z, \eta) d\eta \right], \tag{14}$$

where

$$\begin{aligned} \bar{R}_1^L(s, z, \eta) &= e^{-s(z/\alpha)\sqrt{1+\alpha^2\eta^2}} \frac{k^2}{(1+\eta^2k^2)^{3/2}} \frac{(1+2\beta^2\eta^2)^2}{(1+2\beta^2\eta^2)^2 - 4\frac{\beta^3}{\alpha}\eta^2\sqrt{1+\alpha^2\eta^2}\sqrt{1+\beta^2\eta^2}} \eta, \\ \bar{R}_2^L(s, z, \eta) &= -\frac{4\beta^3}{\alpha} e^{-s(z/\beta)\sqrt{1+\beta^2\eta^2}} \frac{k^2}{(1+\eta^2k^2)^{3/2}} \frac{\eta^2\sqrt{1+\alpha^2\eta^2}\sqrt{1+\beta^2\eta^2}}{(1+2\beta^2\eta^2)^2 - 4\frac{\beta^3}{\alpha}\eta^2\sqrt{1+\alpha^2\eta^2}\sqrt{1+\beta^2\eta^2}} \eta. \end{aligned}$$

In (14), we shall perform the following change of variable in the integrands:

- for $\bar{R}_1^L(s, z, \eta)$: $\frac{z}{\alpha}\sqrt{1+\alpha^2\eta^2} = t, \quad \eta = \frac{\sqrt{\alpha^2t^2 - z^2}}{\alpha z},$
- for $\bar{R}_2^L(s, z, \eta)$: $\frac{z}{\beta}\sqrt{1+\beta^2\eta^2} = t, \quad \eta = \frac{\sqrt{\beta^2t^2 - z^2}}{\beta z}.$

Then the integrals in (14) will take the form

$$R_1^L(s, z) = \int_{z/\alpha}^\infty e^{-st} \tilde{R}_1(t, z) dt, \quad R_2^L(s, z) = \int_{z/\beta}^\infty e^{-st} \tilde{R}_2(t, z) dt.$$

The right-hand term in the latter expressions is the Laplace transform operator; hence, the original in the left-hand side is the integrand function, i.e.,

$$\begin{aligned} R_1(t, z) &= H\left(t - \frac{z}{\alpha}\right) \tilde{R}_1(t, z), \quad \tilde{R}_1(t, z) = -\alpha^3 k^2 \frac{\left[\alpha^2 z^2 + 2\beta^2 \tilde{A}(t, z) \right]^2 t z}{\left[\alpha^2 z^2 + k^2 \tilde{A}(t, z) \right]^{3/2} \Delta_1(t, z)}, \\ R_2(t, z) &= H\left(t - \frac{z}{\beta}\right) \tilde{R}_2(t, z), \quad \tilde{R}_2(t, z) = -4 \frac{\beta^4 k^2 \tilde{B}(t, z) \sqrt{\beta^2 z^2 + \alpha^2 \tilde{B}(t, z)} t^2 z}{\alpha \left[\beta^2 z^2 + k^2 \tilde{B}(t, z) \right]^{3/2} \Delta_2(t, z)}, \end{aligned} \tag{15}$$

where

$$\begin{aligned}\Delta_1(t, z) &= \left[\alpha^2 z^2 + 2\beta^2 \tilde{A}(t, z) \right]^2 - 4\alpha\beta^3 t \tilde{A}(t, z) \sqrt{\alpha^2 z^2 + \beta^2 \tilde{A}(t, z)}, \\ \Delta_2(t, z) &= \left[2\beta^2 t^2 - z^2 \right]^2 - 4\frac{\beta}{\alpha} t \tilde{B}(t, z) \sqrt{\beta^2 z^2 + \alpha^2 \tilde{B}(t, z)}, \\ \tilde{A}(t, z) &= \alpha^2 t^2 - z^2, \quad \tilde{B}(t, z) = \beta^2 t^2 - z^2.\end{aligned}$$

Finally, taking into account the factor $1/s$ in (14), we shall obtain the following exact analytical expression for normal stress $\sigma_{zz}(t, z)$ on the problem's axis of symmetry as integrals of fractional-analytic functions:

$$\sigma_{zz}(t, z) = q_0 \left[H\left(t - \frac{z}{\alpha}\right) \int_{z/\alpha}^t \tilde{R}_1(\tau, z) d\tau + H\left(t - \frac{z}{\beta}\right) \int_{z/\beta}^t \tilde{R}_2(\tau, z) d\tau \right]. \quad (16)$$

Using expressions (10) and (12), and the stated procedure for constructing originals, it is not difficult to obtain an equation for displacement $u_z(t, z)$, which is similar to (16), where

$$\begin{aligned}\tilde{R}_1(t, z) &= \frac{k^2 \alpha^7 z^5 t \left[\alpha^2 z^2 + 2\beta^2 \tilde{A}(t, z) \right] \sqrt{\tilde{A}(t, z)}}{\left[\alpha^2 z^2 + k^2 \tilde{A}(t, z) \right]^{3/2} \Delta_1(t, z)}, \\ \tilde{R}_2(t, z) &= -\frac{2\beta z^3 k^2 \tilde{B}^{3/2}(t, z) \sqrt{\beta^2 z^2 + \alpha^2 \tilde{B}(t, z)}}{\left[\beta^2 z^2 + k^2 \tilde{B}(t, z) \right]^{3/2} \Delta_2(t, z)}.\end{aligned}$$

Let us now consider the load

$$Q(r, t) = q_0 H\left(kt - r^2\right), \quad (17)$$

whose application domain boundary moves with variable velocity. The transform of the function $Q(r, t)$ will have the form

$$Q^{LB}(\xi, s) = q_0 \frac{k}{2s^2} e^{-\xi^2(k/4s)}.$$

Then, (9) yields the following equation for the normal stress transform:

$$\sigma_{zz}^{LB}(\xi, s, z) = q_0 \frac{k}{2s^2} e^{-\xi^2(k/4s)} \frac{\left[(s^2 + 2\beta^2 \xi^2)^2 e^{-(z/\alpha)\sqrt{s^2 + \alpha^2 \xi^2}} - 4\frac{\beta^3}{\alpha} \xi^2 \sqrt{s^2 + \alpha^2 \xi^2} \sqrt{s^2 + \beta^2 \xi^2} e^{-(z/\beta)\sqrt{s^2 + \beta^2 \xi^2}} \right]}{(s^2 + 2\beta^2 \xi^2)^2 - 4\frac{\beta^3}{\alpha} \xi^2 \sqrt{s^2 + \alpha^2 \xi^2} \sqrt{s^2 + \beta^2 \xi^2}}.$$

Applying the same technique as in the previous case, we obtain the following analytical expression for computing the stress σ_{zz} along the problem's axis of symmetry:

$$\sigma_{zz}(t, z) = q_0 \left[H\left(t - \frac{z}{\alpha}\right) F_1(t, z) \frac{\zeta(t, z) - 2z}{\zeta(t, z)} - H\left(t - \frac{z}{\beta}\right) F_2(t, z) \frac{\bar{\zeta}(t, z) - 2z}{\bar{\zeta}(t, z)} \right], \quad (18)$$

where

$$\begin{aligned}F_1(t, z) &= \frac{\left(1 + \frac{8\beta^2}{k^2} f_\alpha(t, z)\right)^2}{\left(1 + \frac{8\beta^2}{k^2} f_\alpha(t, z)\right)^2 - \frac{16\beta^3}{\alpha k^2} f_\alpha(t, z) \sqrt{1 + \frac{4\alpha^2}{k^2} f_\alpha(t, z)} \sqrt{1 + \frac{4\beta^2}{k^2} f_\alpha(t, z)}}, \\ F_2(t, z) &= \frac{16\beta^3}{\alpha k^2} \frac{f_\beta(t, z) \sqrt{1 + \frac{4\alpha^2}{k^2} f_\beta(t, z)} \sqrt{1 + \frac{4\beta^2}{k^2} f_\beta(t, z)}}{\left(1 + \frac{8\beta^2}{k^2} f_\beta(t, z)\right)^2 - \frac{16\beta^3}{\alpha k^2} f_\beta(t, z) \sqrt{1 + \frac{4\alpha^2}{k^2} f_\beta(t, z)} \sqrt{1 + \frac{4\beta^2}{k^2} f_\beta(t, z)}}.\end{aligned}$$

$$f_\alpha(t, z) = tk + 2z^2 - 2z\zeta(t, z), \quad \zeta(t, z) = 2\sqrt{tk + z^2 + \frac{k^2}{4\alpha^2}},$$

$$f_\beta(t, z) = tk + 2z^2 - 2z\bar{\zeta}(t, z), \quad \bar{\zeta}(t, z) = 2\sqrt{tk + z^2 + \frac{k^2}{4\beta^2}}.$$

The expressions for the remaining stresses and displacements are obtained similarly.

4 Numerical-analytic solution

With certain restrictions placed on the investigation time interval, the solution of the problem being considered can be obtained even with an acting load of a sufficiently general kind. So, the analytical solution described previously can serve as a baseline for controlling the accuracy of results. The essence of the method being developed herein consists in the following. Instead of an elastic half-space, we introduce for consideration a certain model elastic semi-infinite cylinder with radius l with such boundary conditions on the lateral surface that the general solution for wave potentials presented as a Fourier–Bessel series fulfills these conditions. Radius l is chosen considering the time interval during which the process should be investigated and the computational procedure for convergence. The solution of this modified problem coincides with the solution of the original problem for half-spaces up to the instant at which waves reflected from the lateral surface occur.

In short, the statement of the modified problem is as follows. With dimensionless notations (1), the solution of wave equations (2) is sought for at zero initial conditions (5), conditions of excitation decay at infinity (at $z \rightarrow \infty$), conditions (4) on the cylinder end (at $z = 0$), and the following conditions on the lateral surface (at $r = l$):

$$\sigma_{rz}|_{r=l} = 0, \quad u_r|_{r=l} = 0. \tag{19}$$

It is assumed that the function $Q(r, t)$, which specifies the pattern of load distribution on the cylinder end, can be expanded into a Fourier–Bessel series on the interval $0 \leq r \leq l$:

$$Q(t, r) = \sum_{n=1}^{\infty} Q_n(t)J_0(\lambda_n r), \quad Q_n(t) = \frac{2}{l^2 J_0(\lambda_n l)^2} \int_0^l Q(r, t)J_0(\lambda_n r)r \, dr. \tag{20}$$

Here, λ_n denotes equation roots:

$$J_1(\lambda_n l) = 0, \quad n = (\overline{1, \infty}). \tag{21}$$

Expansion into a Fourier–Bessel series also exists for stresses and displacements:

$$\sigma_{zz}(r, t, z) = \sum_{n=1}^{\infty} \sigma_{zz_n}(t, z)J_0(\lambda_n r), \quad u_z(r, t, z) = \sum_{n=1}^{\infty} u_{z_n}(t, z)J_0(\lambda_n r),$$

$$\sigma_{rz}(r, t, z) = \sum_{n=1}^{\infty} \sigma_{rz_n}(t, z)J_1(\lambda_n r), \quad u_r(r, t, z) = \sum_{n=1}^{\infty} u_{r_n}(t, z)J_1(\lambda_n r). \tag{22}$$

The general solution for wave equations (2) following application of the Laplace integral transform in time taking into account the zero initial conditions, the decay conditions at infinity, and the conditions (19) on the cylinder lateral surface can be written as

$$\begin{aligned}\Phi^L(r, s, z) &= \sum_{n=1}^{\infty} A_n(s) e^{-(z/\alpha)P} J_0(\lambda_n r), \quad P = \sqrt{s^2 + \alpha^2 \lambda_n^2}, \\ \Psi^L(r, s, z) &= \sum_{n=1}^{\infty} B_n(s) e^{-(z/\beta)S} J_0(\lambda_n r), \quad S = \sqrt{s^2 + \beta^2 \lambda_n^2}.\end{aligned}\quad (23)$$

Here, $A_n(s)$ and $B_n(s)$ are invariables to be defined from boundary conditions (3), which, being subjected to the Laplace transform taking into account expansions (20) and (22), take the form

$$\sigma_{zzn}^L \Big|_{z=0} = Q_n^L(s), \quad \sigma_{rz_n}^L \Big|_{z=0} = 0. \quad (24)$$

By satisfying conditions (24), we obtain expressions for the coefficients of series (22) in transforms for stresses and displacements:

$$\begin{aligned}\sigma_{zzn}^L &= Q_n^L \frac{\alpha(s^2 + 2\beta^2 \lambda_n^2)^2 e^{-(z/\alpha)P} - 4\beta^3 \lambda_n^2 P S e^{-(z/\beta)S}}{\alpha(s^2 + 2\beta^2 \lambda_n^2)^2 - 4\beta^3 \lambda_n^2 P S}, \\ \sigma_{rz_n}^L &= Q_n^L \frac{P(s^2 + 2\beta^2 \lambda_n^2)(e^{-(z/\beta)S} - e^{-(z/\alpha)P})}{\alpha(s^2 + 2\beta^2 \lambda_n^2)^2 - 4\beta^3 \lambda_n^2 P S}, \\ u_{z_n}^L &= Q_n^L \frac{P[-\alpha(s^2 + 2\beta^2 \lambda_n^2)e^{-(z/\alpha)P} + 2\beta^2 \lambda_n^2 e^{-(z/\beta)S}]}{\alpha(s^2 + 2\beta^2 \lambda_n^2)^2 - 4\beta^3 \lambda_n^2 P S}, \\ u_{r_n}^L &= Q_n^L \frac{\alpha \lambda_n (s^2 + 2\beta^2 \lambda_n^2) e^{-(z/\alpha)P} - 2\beta^2 P S e^{-(z/\beta)S}}{\alpha(s^2 + 2\beta^2 \lambda_n^2)^2 - 4\beta^3 \lambda_n^2 P S}.\end{aligned}$$

Now the problem consists of the inversion of the expressions obtained and summing the series. This procedure can be shown by the example of computing the stress σ_{zz} . Let us present σ_{zzn}^L as

$$\sigma_{zzn}^L = Q_n^L(s) D_n^L(s, z), \quad D_n^L(s, z) = \frac{\alpha(s^2 + 2\beta^2 \lambda_n^2)^2 e^{-(z/\alpha)P} - 4\beta^3 \lambda_n^2 P S e^{-(z/\beta)S}}{\alpha(s^2 + 2\beta^2 \lambda_n^2)^2 - 4\beta^3 \lambda_n^2 P S}. \quad (25)$$

If the original $D_n(t, z)$ is found, then $\sigma_{zzn}(t, z)$ can be determined using the convolution [19]

$$\sigma_{zzn} = \int_0^t Q_n(\tau) D_n(t - \tau, z) d\tau. \quad (26)$$

To find the original, $D_n^L(s, z)$ is rewritten as follows:

$$\begin{aligned}D_n^L(s, z) &= \left\{ e^{-(z/\alpha)s} + \left(e^{-(z/\alpha)P} - e^{-(z/\alpha)s} \right) + \frac{4\beta^3 P S \lambda_n^2}{\alpha(s^2 + 2\lambda_n^2 \beta^2)^2 - 4\beta^3 \lambda_n^2 P S} \right. \\ &\quad \left. \times \left[\left[e^{-(z/\alpha)s} + \left(e^{-(z/\alpha)P} - e^{-(z/\alpha)s} \right) \right] - \left[e^{-(z/\beta)s} + \left(e^{-(z/\beta)S} - e^{-(z/\beta)s} \right) \right] \right] \right\}. \quad (27)\end{aligned}$$

Use the notation

$$R_n^L(s) = \frac{4\beta^3 P S \lambda_n^2}{\alpha(s^2 + 2\lambda_n^2 \beta^2)^2 - 4\beta^3 P S \lambda_n^2} = \frac{F_n^L(s)}{1 - F_n^L(s)}, \quad (28)$$

where

$$F_n^L(s) = \frac{4\beta^3 P S \lambda_n^2}{\alpha (s^2 + 2\lambda_n^2 \beta^2)^2},$$

and rewrite (28) as

$$(1 - F_n^L(s))R_n^L(s) = F_n^L(s). \tag{29}$$

Expression (29) in the space of originals is the integral Volterra equation of the second kind:

$$R_n(t) - \int_0^t R_n(\tau)F_n(t - \tau)d\tau = F_n(t). \tag{30}$$

The function $F_n(t) = L^{-1}\{F_n^L(s)\}$ is determined as follows:

$$F(t) = L^{-1}\left\{\frac{4\lambda_n^2\beta^3}{\alpha} \frac{s(s^2 + \alpha^2\lambda_n^2)}{(s^2 + 2\lambda_n^2\beta^2)^2} \frac{S}{sP}\right\} = L^{-1}\left\{\frac{4\lambda_n^2\beta^3}{\alpha} l_1^L(s)l_2^L(s)\right\}. \tag{31}$$

Originals l_1 and l_2 have the following form [19]:

$$\begin{aligned} l_1(t) &= L^{-1}\left\{\frac{s(s^2 + \alpha^2\lambda_n^2)}{(s^2 + 2\lambda_n^2\beta^2)^2}\right\} \\ &= \cos(\sqrt{2}\beta\lambda_n t) + \frac{\sqrt{2}\lambda_n(\alpha^2 - 2\beta^2)}{4\beta} t \sin(\sqrt{2}\beta\lambda_n t), \\ l_2(t) &= L^{-1}\left\{\frac{S}{sP}\right\} = L^{-1}\left\{\frac{1}{s\sqrt{s^2 + \alpha^2\lambda_n^2}}\left(\sqrt{s^2 + \beta^2\lambda_n^2} - s\right) + \frac{1}{\sqrt{s^2 + \alpha^2\lambda_n^2}}\right\} \\ &= \beta\lambda_n \int_0^t J_{i_0}[\alpha\lambda_n(t-\tau)]\frac{1}{\tau} J_1(\beta\lambda_n \tau)d\tau + J_0(\alpha\lambda_n t), \quad J_{i_0}(\alpha\lambda_n t) = \int_0^t J_0(\alpha\lambda_n \tau)d\tau. \end{aligned}$$

Applying convolution to (31) gives the following expression in the space of the originals

$$F_n(t) = \frac{4\lambda_n^2\beta^3}{\alpha} \int_0^t l_1(t - \tau)l_2(\tau)d\tau. \tag{32}$$

We shall also use known inversion formulas [19] to find the originals of the functions in (27), namely,

$$L^{-1}\left\{e^{-(z/\alpha)P} - e^{-(z/\alpha)S}\right\} = k_{n\alpha}(t, z) = -H\left(t - \frac{z}{\alpha}\right)z\lambda_n \frac{J_1\left(\alpha\lambda_n\sqrt{t^2 - (z/\alpha)^2}\right)}{\sqrt{t^2 - (z/\alpha)^2}}, \tag{33}$$

$$L^{-1}\left\{e^{-(z/\beta)S} - e^{-(z/\beta)P}\right\} = k_{n\beta}(t, z) = -H\left(t - \frac{z}{\beta}\right)z\lambda_n \frac{J_1\left(\beta\lambda_n\sqrt{t^2 - (z/\beta)^2}\right)}{\sqrt{t^2 - (z/\beta)^2}}. \tag{34}$$

Finally, the original $D_n(t, z)$ can be written as

$$D_n(t, z) = \delta(t - z/\alpha) + \tilde{K}_n(t, z), \quad (35)$$

where $\delta(t)$ is the Dirac delta function, and the function $\tilde{K}_n(t, z)$ is such that its transform $\tilde{K}_n^L(s, z)$ has the form

$$\begin{aligned} \tilde{K}_n^L(s, z) &= k_{n\alpha}^L + R_n^L \left\{ \left[e^{-(z/\alpha)s} + k_{n\alpha}^L \right] - \left[e^{-(z/\beta)s} + k_{n\beta}^L \right] \right\} \\ &= k_{n\alpha}^L + e^{-(z/\alpha)s} R_n^L - e^{-(z/\beta)s} R_n^L + R_n^L \left[k_{n\alpha}^L - k_{n\beta}^L \right]. \end{aligned}$$

Hence, the original $\tilde{K}_n(t, z)$, taking into account the operational calculus lag and multiplication theorems, is written as follows:

$$\begin{aligned} \tilde{K}_n(t, z) &= k_{n\alpha}(t, z) + H\left(t - \frac{z}{\alpha}\right) R_n\left(t - \frac{z}{\alpha}\right) - H\left(t - \frac{z}{\beta}\right) R_n\left(t - \frac{z}{\beta}\right) \\ &\quad + \int_0^t R_n(t - \tau) [k_{n\alpha}(\tau, z) - k_{n\beta}(\tau, z)] d\tau. \end{aligned} \quad (36)$$

Note that $R_n(t)$ is the solution of integral equation (30), and functions $k_{n\alpha}(t, z)$ and $k_{n\beta}(t, z)$ are specified by expressions (33) and (34).

Formulas (26) and (35) yield an expression for σ_{zzn}

$$\sigma_{zzn}(t, z) = H\left(t - \frac{z}{\alpha}\right) Q_n\left(t - \frac{z}{\alpha}\right) + \int_0^t Q_n(\tau) \tilde{K}_n(t - \tau, z) d\tau. \quad (37)$$

Finally, the normal stress is determined by the formula

$$\begin{aligned} \sigma_{zz}(r, t, z) &= \sum_{n=1}^{\infty} \sigma_{zzn}(t, z) J_0(\lambda_n r) \\ &= H\left(t - \frac{z}{\alpha}\right) Q\left(t - \frac{z}{\alpha}, r\right) + \sum_{n=1}^{\infty} J_0(\lambda_n r) \int_0^t Q_n(\tau) \tilde{K}_n(t - \tau, z) d\tau. \end{aligned} \quad (38)$$

A procedure similar to that described earlier is used to compute the remaining components of the deflected mode.

5 Numerical results

Let us offer some numerical results obtained both based on the exact analytical expressions described in Sect. 2 and with the help of the numerical-analytic technique described in the previous section. In so doing, we chose the following values of parameters of a half-space's material: $\alpha = 1.0$ and $\beta = 0.55$. It should be noted that the coefficient β determines Poisson's ratio ν of the half-space's material. Thus, using the equations $\beta = c_s/c_p$, $c_p = \sqrt{(\lambda + 2\mu)/\rho}$, and $c_s = \sqrt{\mu/\rho}$ (λ and μ are Lamé's elastic constants), it is not difficult to obtain the equation for $\nu - \nu = (1 - 2\beta^2)/(2 - 2\beta^2)$. And the accepted value $\beta = 0.55$ corresponds to $\nu = (1 - 2 \cdot 0.55^2)/(2 - 2 \cdot 0.55^2) \approx 0.283$. It was assumed that the load acting on the surface $z = 0$ had the form

$$Q(r, t) = q_0 H(t) H(r^* - |r|), \quad (39)$$

where $q_0 = -1$. The radius of the model cylinder l was set equal to π (Fig. 1).

When computing the stress σ_{zz} using the analytical expression (16), as well as when solving the integral equation (30) and computing the integrals in (26), (32), and (36)–(38), we used Simpson quadrature formulas. The constant integration step Δt , as well as the number of terms N retained in the Fourier–Bessel series in (38), was chosen to

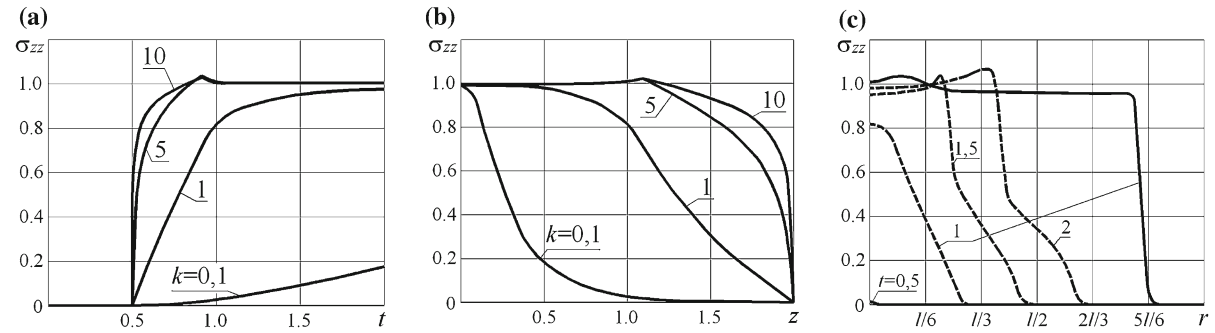


Fig. 2 Stresses $\sigma_{zz}(r, t, z)$ at $Q(r, t) = q_0 H(t) H(\tilde{k}t - |r|)$ with different \tilde{k} . **a** σ_{zz} at point $(r = 0, z = 0.5)$, **b** σ_{zz} on z -axis at moment $t = 2$, **c** σ_{zz} in section $z = 0.5$ at fixed t for $\tilde{k} = 1$ and 5

satisfy the condition of providing the required computational accuracy. Thus, the difference in the maximum values of both the stress σ_{zz} (38) and the function R_N (30) on the time interval being investigated $[0, T]$ ($T = 2$) at $N = 80$ and $\Delta t = 1/5000$ and $\Delta t = 1/8000$ was within 1%.

The convergence of the Fourier–Bessel series was accelerated using the factors $\phi_n = 2J_1(\varphi_n)/\varphi_n$, where $\varphi_n = \lambda_2 l(n - 1)/(N - 1)$, and λ_2 is the least positive root of the equation $J_1(\lambda_2 l) = 0$.

When using the quadrature method for computing integrals containing the function $k_{n\alpha}$ with a finite discontinuity point $t = t_\alpha = z/\alpha$ ($k_{n\alpha}(t, z)|_{t < t_\alpha} \equiv 0$; $\lim_{\delta \rightarrow 0} k_{n\alpha}(t_\alpha + \delta, z) = -z\alpha\lambda_n^2/2$), integration along the interval $(t'_\alpha; t'_\alpha + \Delta t)$ containing this point involved integrating along the subinterval of nonzero values of $k_{n\alpha}$. Here, $t'_\alpha = \Delta t \cdot E(t_\alpha/\Delta t)$, where $E(x)$ is the integer part of the argument. A similar procedure was used to compute integrals with an integrand $k_{n\beta}(t, z)$.

Figures 2 and 3 show the case where the acting load propagates over the half-space surface with a definite velocity, viz. a constant velocity, at which the boundary of the load distribution domain is defined by the radius $r^*(t) = \tilde{k}t$ (Fig. 2) and a variable velocity when the given radius equals $r^*(t) = \sqrt{\tilde{k}t}$ (Fig. 3). Figure 2a shows the time-dependent development of the stress σ_{zz} on the z -axis at the point $r = 0, z = 0.5$ for several values of the velocity parameter $k = \tilde{k}/\alpha$: $k = 0.1, 1, 5, 10$. Here, and in the following figures, stress relates to the amplitude of the acting load q_0 . In the point considered, stress occurs with the arrival of a compression wave ($t = z/\alpha = 0.5$), and subsequently tends to unit. At that point, the rate at which a stationary value is achieved depends significantly on the value of k . With small values of k ($k = 0.1; 1$), the stress grows quite slowly, whereas with k equal to 5 or 10, the stress at the instant of arrival of the stress wave front increases stepwise and rapidly achieves the ultimate value occurring at the instant when the shear wave point ($t = z/\beta \approx 0.909$) is achieved.

Figure 2b shows the stress distribution along the z -axis ($r = 0$) at a fixed point in time $t = T$ for the same values of the velocity parameter k . Here, we also see the significant dependence of the stress distribution profile on the given parameter. In the figure, for $k = 5$ and 10 , one observes the location of the shear wave front, which shows a break in the corresponding graphs ($z = \beta T = 1.1$). Note that the graphs in Fig. 2b were computed using both the analytical solution in Sect. 2 and with the help of the developed numerical-analytic procedure described in Sect. 3. In this way, it turned out that the results obtained agree to within the graph thickness. This confirms the practical accuracy of the numerical-analytic procedure and allows us to use it, for instance, to calculate the stress distribution along the Or -axis. In particular, Fig. 2c shows the distribution of σ_{zz} in the section $z = 0.5$ at fixed time instants $t = z/\alpha = 0.5, 1, 1.5, T = 2$ computed in such a manner. The dashed lines show the graphs for $k = 1$ and the solid lines show them for $k = 5$. For the previous value of k , the stress graphs for $t = 1.5, 2$ are not shown because this case shows the influence of an artificially introduced boundary of the model cylinder, which distorts the computations.

Figure 3 shows the process being investigated when the boundary of the load action domain is defined by the function $r^*(t) = \sqrt{\tilde{k}t}$. The results shown in Fig. 3a, b were obtained for velocity parameter values of $k = \tilde{k}/\alpha = 0.1, 1, 5, 10$. Figure 3a shows stress as a time function at a particular point ($r = 0, z = 0.5$); Fig. 3b shows it as a

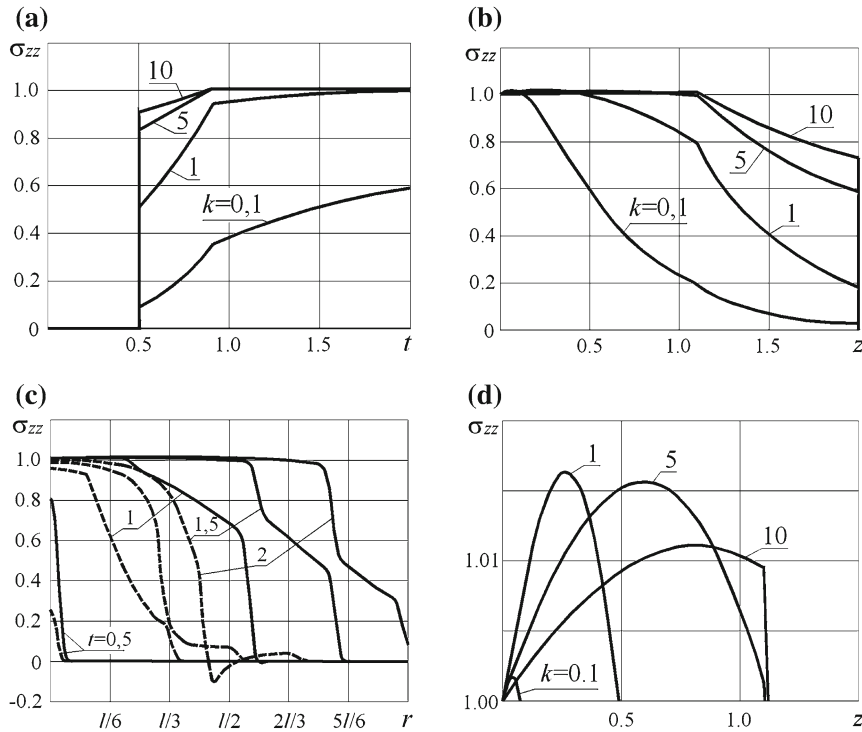


Fig. 3 Stresses $\sigma_{zz}(r, t, z)$ at $Q(r, t) = q_0 H(t) H(\tilde{k}t - r^2)$ with different \tilde{k} . **a** σ_{zz} at point $(r = 0, z = 0.5)$, **b** σ_{zz} on z -axis at moment $t = 2$, **c** σ_{zz} in section $z = 0.5$ at fixed t for $\tilde{k} = 1$ and 5 , and **d** increased fragment of Fig. 3b

function of z on the symmetry axis ($r = 0$) at the time point $t = T$. In these figures, one can see the position and influence (as a graph break) of the shear wave front. Note again that the preceding graphs were obtained using both analytical and numerical-analytic procedures, and the computation results were in very good agreement. Figure 3c was built using the technique in Sect. 3. It shows the stress distribution along radius r at fixed time points $t = 0.5, 1, 1.5, 2$ for values of parameter k equal to 1 (the dotted graph) and 5 (the solid graph). Note that the graph $t = 2, k = 5$ was obtained taking into account the model cylinder boundary influence. The position of the shear wave in the section and, hence, at the time the boundary $r = l$ was reached can be computed approximately using formula $\tilde{r} + \sqrt{(\alpha(t - t_r))^2 - z^2}$, where t_r is the time point at which the radius of the load action domain becomes equal to \tilde{r} ($\tilde{r} \leq r^*(t)$), whereas \tilde{r} is taken such as to obtain a maximum value for the given formula. By replacing α with β , one can obtain the shear wave position similarly. The computed values for the points of intersection of compression and shear waves with the plane $z = 0.5$ for $k = 5$ at $t = 2$ were approximately $5.93l/6$ and $4.72l/6$. This is in good agreement with the graph in Fig. 3c.

Let us note that Fig. 3b's scale does not allow us to observe the following singularity of distribution of the stress along the z -axis: at any value of k there is the axis segment z on which the stress σ_{zz} exceeds the value preset on the surface $z = 0$. This is clearly visible in Fig. 3d, which is drawn in a corresponding scale. This singularity is apparently caused by the circumstance that for load (39) with $r^*(t) = \sqrt{\tilde{k}t}$ there is always a time interval in which the boundary of the load distribution's area moves at a velocity exceeding the pressure wave's velocity. Incidentally, in the case of load (39) with $r^*(t) = \tilde{k}t$, such excess takes place at $k > 1$, as noticed in Fig. 2b.

Finally, Fig. 4 shows the results of numerical-analytic computations for the case where the load distribution along the radial coordinate is defined by the expression $q_0 \sqrt{1 - (r/r^*)^2}$, whereas the radius of its action domain is fixed ($r^* = l/6$) or changes with a constant or variable velocity [$r^*(t) = l/6 + \tilde{k}t$ or $r^*(t) = l/6 + \sqrt{\tilde{k}t}$; $\tilde{k} = k\alpha = 1$]. Figure 4a shows stress development at the point $(r = 0, z = 0.5)$; Fig. 4b shows the distribution of stress σ_{zz} along

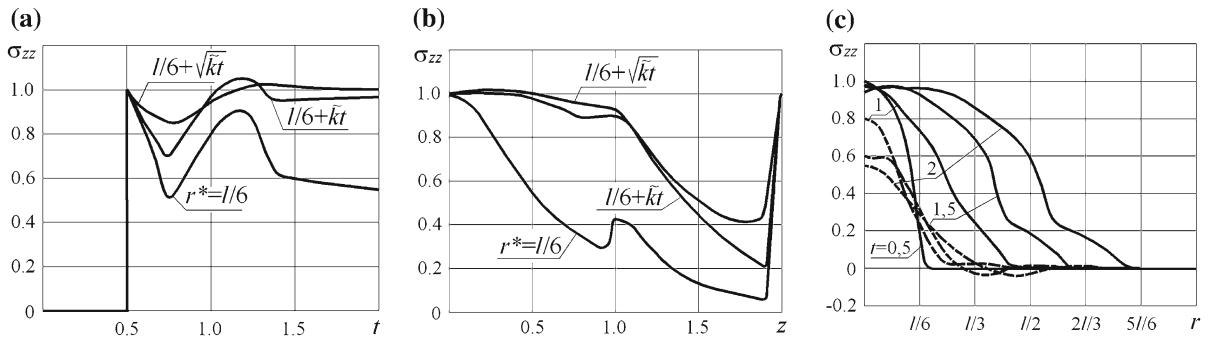


Fig. 4 Stresses $\sigma_{zz}(r, t, z)$ at $Q(r, t) = q_0\sqrt{1 - (r/r^*(t))^2}H(t)H(r^*(t) - |r|)$ with different $r^*(t)$. **a** σ_{zz} at point $(r = 0, z = 0.5)$, **b** σ_{zz} on z -axis at moment $t = 2$, and **c** σ_{zz} in section $z = 0.5$ at fixed t for $r^* = l/6$ and $r^* = l/6 + \tilde{k}t$

the Oz -axis ($r = 0$) at the time point $t = T = 2$; Fig. 4b shows the stress distribution along the Or -axis in the section $z = 0.5$ at time points $t = 0.5, 1, 1.5$, and 2 (the dotted graph shows the results for $r^* = l/6$, and the solid lines show those for $r^* = l/6 + \tilde{k}t$).

Figure 4a shows that, with the arrival of the compression wave at the point considered ($t = z/\alpha = 0.5$), the stress σ_{zz} grows stepwise to unit and then drops and takes a minimal value with the arrival at the point of an expansion wave propagating from the edge of the load application domain ($t = \sqrt{z^2 + (r^*)^2}/\alpha \approx 0.724$). With a movable load boundary (graphs $l/6 + \tilde{k}t$ and $l/6 + \sqrt{\tilde{k}t}$), this effect becomes more fuzzy. The impact of the shear wave, whose front passes through the given point at $t = z/\beta \approx 0.909$, is practically negligible. The figure also shows that, after the shear wave has passed from the edge of the load application domain ($t = \sqrt{z^2 + (r^*)^2}/\beta \approx 1.316$), the stress changes smoothly.

Figure 4b makes it possible to evaluate the influence of the velocity of the load domain boundary motion on the stress distribution profile along the Oz -axis at $t = T = 2$. The graph corresponding to the fixed boundary clearly shows the positions of wave fronts, viz. compression–expansion waves $z = \alpha T = 2$ and $z = \sqrt{(\alpha T)^2 - (r^*)^2} \approx 1.93$, and shear waves $z = \beta T = 1.1$ and $z = \sqrt{(\beta T)^2 - (r^*)^2} \approx 0.967$. At a moving load domain boundary, behind the expansion wave front one can also see a sharp stress drop followed by its growth to a value of 1 acting on the surface. Behind the shear wave front, there is practically no area with a sharp stress drop.

To evaluate the effectiveness of the numerical-analytic method and the validity of the results obtained, we also considered the case of applying a finite unit pulse ($Q(r, t) = H(T^* - t)H(r^* - r)$) evenly distributed in a circle with radius $r^* = \text{const}$, which was studied in [6, 14]. Graph 3 in Fig. 5a, showing the distribution of the stress σ_{zz} along the Oz -axis at $t = 2$, was computed using the method described herein and the initial data given in the aforementioned publications ($\alpha = 1; \beta = 1/\sqrt{3}; T^* = 0.5; r^* = 0.5$), whereas graph 1 was obtained using the integral transform method [14], and graph 2 was obtained using the finite-difference method [6]. The causes of the sharp stress value changes (Fig. 5a) are set forth in detail in [14].

This problem was also solved using bundled software employing the finite-element method. The implicit two-parameter ($\xi = (1 + \zeta)^2/4; \psi = 1/2 + \zeta$) Newmark method with $\zeta = 0.1$ was used for numerical integration of the calculation equation set. It should be noted that this scheme with standard parameter values ($\zeta = 0$) refers to dissipationless methods that lead to an occurrence of parasitic oscillations in numerical solutions of problems on wave distributions in solids under shock loadings [20]. The result of the finite-element modeling as the stress σ_{zz} at the point $(r = 0, z = 0.5)$ when the load $Q(r, t) = H(T^* - t)H(r^* - r)$ is on the end surface of the modeling cylinder is presented in Fig. 5b as dashed curve 1 ($T^* = 0.5; r^* = 0.5$). The sizes of the finite elements of the discrete model, including those near the researched point, their degree, time-step sizes, and the parameter ζ , were chosen from conditions of solution stability and integration accuracy. From a comparison of dashed curve 1 and continuous curve 2 [the latter is calculated on the basis of expression (38)], it is possible to draw a conclusion

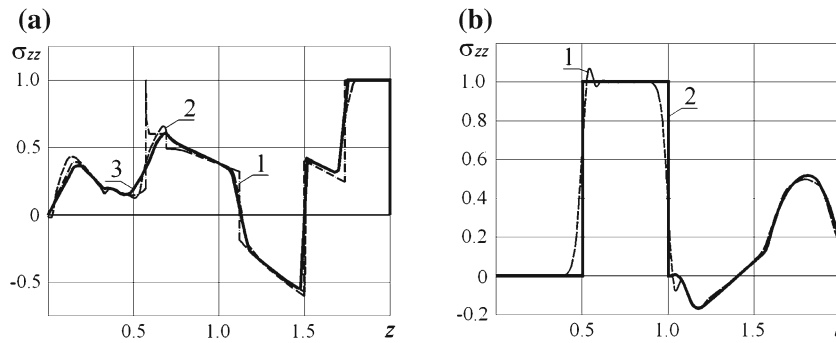


Fig. 5 Validation of developed method by stress σ_{zz} calculated at $Q(r, t) = H(0.5 - t)H(0.5 - r)$. **a** σ_{zz} on z -axis at moment $t = 2$ and **b** σ_{zz} at point ($r = 0, z = 0.5$)

on the topicality of the investigations dedicated to the development of effective analytical approaches to studying nonstationary processes, especially in case of impulse-type loadings.

6 Conclusions

This paper describes a numerical-analytic method of solving the problem of the action on an elastic half-space of an axisymmetric nonstationary mechanical load distributed arbitrarily in a domain with a variable boundary. The method is built around the time-variable Laplace transform and expansion into the Fourier–Bessel series for the radial coordinate of a model cylinder. This made it possible to eliminate the inversion of two integral transforms. Inversion of the Laplace transform by a series of successive manipulations makes the solution yield stepwise functions. As for the remaining smoother part, the inversion problem is reduced to solving a series of integral Volterra equations of the second kind.

To investigate processes in an elastic half-space that are due to the application to its boundary of an axisymmetric load evenly distributed in a circle with a boundary expanding at a constant or variable velocity, an analytical approach was developed and described. It involves the use of Laplace and Hankel integral transforms with subsequent application of the Cagniard–de Hoop technique for transition to the domain of originals to obtain exact analytical expressions for stresses and displacements in points along the axis of symmetry of the problem.

Some results of the numerical-analytic method were compared with solutions obtained using the analytical method described, with solutions obtained by other authors, as well as with those computed using the finite-element method. Agreement of numerical-analytic and analytical results confirms the practical accuracy of the methods described and is indicative of their effectiveness for studying the dynamics of elastic media in cases where arbitrarily distributed axisymmetric loads are applied.

7 Summary

The present study considers the axisymmetric problem of determining the stressed state of an elastic half-space to whose boundary a nonstationary load is applied in the form of normal stress. Analytical and numerical-analytic approaches are developed for its solution. In the first case, Laplace and Hankel integral transforms are used. Their inversion is performed jointly, and as a result, an exact solution of the problem is obtained, and stresses along the problem axis of symmetry are found. In the second case, the Laplace integral transform with inversion into a Fourier–Bessel series is used. This reduces the problem to solving a series of integral Volterra equations. The approaches developed make it possible to compute the parameters of the deflected mode of a half-space with controlled accuracy. Examples of numerical computations are given.

References

1. De A, Roy A (2012) Transient response of an elastic half-space to normal pressure acting over a circular area on an inclined plane. *J Eng Math* 74:119–141
2. Gorshkov AG, Tarlakovskii DV (1995) Dynamic contact problems with moving boundaries. FIZMATLIT, Moscow, 352 p [in Russian]
3. Kubenko VD, Marchenko TA (2004) Axisymmetric collision problem for two identical elastic solids of revolution. *Int Appl Mech* 40:766–775
4. Kubenko VD, Ocharovich G, Ayzenberg-Stepanenko MV (2011) Impact indentation of a rigid body into an elastic layer; axisymmetric problem. *J Math Sci* 176:670–687
5. Alexandrov VM, Vorovich II (2001) Mechanics of contact interactions. FIZMATLIT, Moscow, 672 p [in Russian]
6. Lin X, Ballmann J (1995) A numerical scheme for axisymmetric elastic waves in solids. *Wave Motion* 21:115–126
7. Laturelle FG (1989) Finite element analysis of wave propagation in an elastic half-space under step loading. *Comput Struct* 32:721–735
8. Molotkov LA (1967) On the vibrations of a homogeneous elastic half-space under the action of a source applied to a uniformly expanding circular region. *J Appl Math Mech* 31:232–243
9. Roy A (1979) Response of an elastic solid to non-uniformly expanding surface loads. *Int J Eng Sci* 17:1023–1038
10. Kutzenko AG, Ulitko AF, Oliynik VN (2001) Displacements of the elastic half-space surface caused by instantaneous axisymmetric loading. *Int J Fluid Mech Res* 28:258–273
11. Ghosh SC (1970) Disturbance produced in an elastic half-space by impulsive normal pressure. *Pure Appl Geophys* 80:71–83
12. Mitra M (1964) Disturbance produced in an elastic half-space by impulsive normal pressure. *Math Proc Camb Philos Soc* 60:683–696
13. Duffy DG (2004) Transform methods for solving partial differential equations. Chapman & Hall/CRC Press, New York, 728 p
14. Laturelle FG (1991) The stresses produced in an elastic half-space by a pressure pulse applied uniformly over a circular area: role of the pulse duration. *Wave Motion* 14:1–9
15. Bresse LF, Hutchins DA (1989) Transient generation of elastic waves in solids by a disk-shaped normal force source. *J Acoust Soc Am* 86:810–817
16. Singh SK, Kuo JT (1970) Response of an elastic half-space to uniformly moving circular surface load. *Trans ASME J Appl Mech* 37:109–115
17. Kubenko VD (2004) Impact of blunted bodies on a liquid or elastic medium. *Int Appl Mech* 40:1185–1225
18. Guz' AN, Kubenko VD, Cherevko MA (1978) Diffraction of elastic waves. *Sov Appl Mech* 14:789–798
19. Bateman H, Erdélyi A (1954) Tables of integral transforms [in two volumes]. McGraw-Hill, New York
20. Wang Y-C, Murti V, Valliappan S (1992) Assessment of the accuracy of the Newmark method in transient analysis of wave propagation problems. *Earthq Eng Struct Dyn* 21:987–1004